Active Site Mutant Glu-43 → Asp in Staphylococcal Nuclease Displays Nonlocal Structural Changes†,‡

Patrick J. Loll

Department of Biochemistry and Molecular Biology, University of Chicago, 920 E. 58th Street, Chicago, Illinois 60637

Eaton Edward Lattman*

Department of Biophysics, Johns Hopkins Medical School, Baltimore, Maryland 21205-2185

Received February 13, 1990; Revised Manuscript Received April 11, 1990

ABSTRACT: The crystal structure of the Glu-43 → Asp mutant of staphylococcal nuclease complexed with Ca^{2+} and the inhibitor thymidine 3′,5′-bisphosphate (pdTp) has been determined and refined by restrained least-squares methods to a conventional crystallographic R value of 0.174 at a resolution of 1.74 Å. Throughout most of the structure, the conformation of the backbone atoms of the mutant is similar to that of the wild-type protein; however, the seemingly conservative mutation Glu → Asp has significantly perturbed the structure of a loop adjacent to the active site, as well as giving rise to looser binding of the essential calcium ion and to a less extensive network of bound water molecules in the active site. Crystal contacts that extend into the active site have also been altered by this amino acid substitution. The changes caused by this mutation are considerably more drastic than would have been predicted and should serve as caveats to those who would draw conclusions about structure–function relationships on the basis of site-directed mutagenesis experiments in the absence of structural data.

Site-directed mutagenesis techniques have revolutionized the study of protein structure and function, enabling experimenters to alter amino acid sequences and observe the effects of these changes upon the resulting mutant molecules. Structural information about mutant proteins, such as may be obtained from X-ray crystallography or nuclear magnetic resonance (NMR) methods, has been accumulating, albeit at a rate much slower than that at which mutants are being produced. High-resolution X-ray structures of a number of mutant proteins, including mutants of T4 lysozyme, dihydrofolate reductase, and subtilisin, have demonstrated that an altered side chain can be incorporated into a folded structure with little or no structural perturbation beyond the immediate vicinity of the side chain. It is tempting, then, to use a minimalist approach in interpreting functional changes observed in mutant proteins, ascribing the changes in activity or stability solely to local changes around the modified side chain, while assuming that the rest of the polypeptide has not been changed.

New evidence suggests, however, that it is not safe to generalize from the examples mentioned above to all mutant proteins. Specifically, we have determined and refined the structure of the Glu-43 → Asp mutant of staphylococcal nuclease (nuclease E43D) at atomic resolution and compared it to the refined wild-type structure. An important and unexpected result emerges from this structure determination: Changing residue 43 from a glutamate to an aspartate gives rise to many small but significant changes in the structure of the active site and drastically alters the conformation of a loop adjacent to the active site.

Materials and Methods

Protein Purification and Crystal Growth. Nuclease E43D was purified from a strain of *Escherichia coli* carrying a mutated form of the plasmid pONF1, kindly supplied by Dr. John Gerlt (Takahara et al., 1985). Induction of protein synthesis was carried out as described (Hibler et al., 1987); protein was isolated and purified as described for wild-type nuclease (Loll & Lattman, 1989). Crystals of the complex of nuclease E43D, Ca^{2+}, and pdTp[1] were grown according to the same vapor diffusion technique as described for wild-type nuclease (vide supra), although the specific conditions differed from those used for wild type. MPD was added to a 25.5 $mg \cdot mL^{-1}$ solution of nuclease E43D in 10.5 mM potassium phosphate, pH 8.15, to a final concentration of 22.6% MPD (w/w); this solution was incubated at 4 °C as per wild type. After incubation, 2.3 molar equiv of pdTp (as a 4 $mg \cdot mL^{-1}$ solution in water) and 2.0 molar equiv of calcium (as 10 mM $CaCl_2$, 20 mM potassium citrate) were added, the solution was filtered, and drops were placed on siliconized cover slips inverted over wells containing 28–30% MPD (w/w) in 10.5 mM potassium phosphate, pH 8.15. Large single crystals grew at 4 °C in 1–2 weeks. These crystals proved to be isomorphous with wild-type crystals, having the space group $P4_1$, with unit-cell constants $a = b = 48.59$ Å and $c = 63.38$ Å.

Data Collection and Reduction. Two data sets were used in the refinement of this structure. The first was collected on film, by use of oscillation photography, from three crystals at the protein crystallography beamline at the National Synchrotron Light Source (Brookhaven National Laboratory); films were processed at a national facility at Purdue University. These data were merged with a low-resolution (12–2.8 Å) diffractometer data set by use of the crystallographic software

† Supported by Grant GM-36385-03 from the National Institutes of Health.

‡ Coordinates of the refined wild-type and E43D mutant structures, as well as structure factors used in determining these structures, have been deposited with the Protein Data Bank, Chemistry Department, Brookhaven National Laboratories, Upton, Long Island, NY 11973.

* Author to whom correspondence should be addressed.

[1] Abbreviations: pdTp, thymidine 3′,5′-bisphosphate; MPD, 2-methyl-2,4-pentanediol; rms, root mean-square.

0006-2960/90/0429-6866$02.50/0 © 1990 American Chemical Society

Table I: Parameters of the Refined E43D Structure

total no. of atoms	1168
no. of solvent atoms	60
mean isotropic B value (Å^2)	31.2
overall anisotropic ΔB (Å^2)[a]	
b_{11}	2.4
b_{22}	1.3
b_{33}	−3.7
RMS deviations from ideal geometry	
bond distances (Å)	0.025
angle distances (Å)	0.065
1–4 distances (Å)	0.073
planarity (Å)	0.023
overall bond angles (deg)	3.6
chiral vol (Å^3)	0.24
isotropic thermal factor restraints (Å^2)	
main-chain bonds	1.5
side-chain bonds	2.0

[a] See Sheriff and Hendrickson (1987).

package PROTEIN (Steigemann, 1974), yielding a data set that is 76% complete in the resolution range 12–1.68 Å and has a merging R value of 0.102 for intensities. After refinement results obtained with this data set proved unsatisfactory, a second data set was collected by use of Xentronics multiwire area detector mounted on a Huber goniostat. Data frames were processed with the XENGEN software package (Howard et al., 1987), yielding a data set that is 80% complete in the resolution range 12–1.74 Å and has a merging R value of 0.051 for intensities. Howard has suggested calculating the mean values of reflections' intensities divided by the standard deviations of their intensities in shells of resolution as a means of objectively measuring the resolution of macromolecular diffraction data sets (A. J. Howard, personal communication); the resolution at which this mean ratio falls below 2 would then be taken as the nominal resolution of the data set. Attempts to calculate this parameter for both of these data sets were unsuccessful, as the mean ratio of I/σ never dropped below 2.0, even at the highest resolution measured.

Refinement. At the time this refinement was begun, the refinement of the structure of the ternary complex of wild-type nuclease, Ca^{2+}, and pdTp was not complete. For this reason, and also to minimize the likelihood of introducing bias into the refinement of the mutant structure, the starting model for the refinement was derived from the wild-type structure (Cotton et al., 1977) found in the Protein Data Bank. The refinement program used was PROLSQ (Hendrickson, 1985), and the strategy employed was similar to that used for the wild-type structure (Loll & Lattman, 1989). Briefly, rounds of rebuilding and solvent molecule placement were alternated with rounds of successive cycles of PROLSQ. Solvent molecules were placed in the model only if density was observed in both $2F_o - F_c$ and ΔF maps[2] and only if they could participate in hydrogen bonds with reasonable geometry. The refinement was judged to have converged after 174 cycles with a crystallographic residual of 0.19 for all data in the resolution range 6–1.68 Å having $F_o/\sigma > 3.0$. We were not satisfied with the results of this refinement; the residual was significantly higher than that obtained with the wild-type structure, and more importantly, the final electron density map was not sufficiently clear to enable us to resolve certain structural features with confidence. Accordingly, we collected the second data set. The model derived from 174 cycles of PROLSQ using the first data set was refined against this second data set.

[2] $2F_o - F_c$ and ΔF maps: maps computed by Fourier syntheses using amplitudes of $|2F_o - F_c|$ and $|F_o - F_c|$, respectively, and phases calculated from the model.

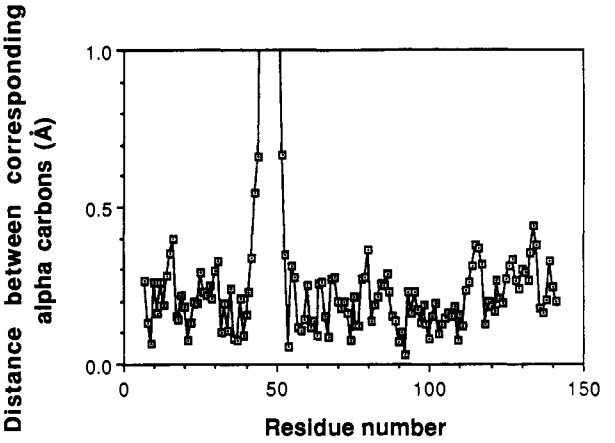

FIGURE 1: Distance between corresponding α-carbon positions in the refined wild-type and nuclease E43D ternary complex structures. The E43D structure was superimposed upon that of the wild type as described in the text before computation of distances.

Simulated annealing was conducted with the XPLOR program package (Brunger, 1988, 1989), running on either a VAX 8530 computer or the Cray XMP supercomputer at the National Cancer Institute. The model was subjected to rigid body refinement, followed by heating and slow cooling. The post-XPLOR model displayed a crystallographic R value of 0.22 for data between 20 and 1.74 Å. This model was further refined with PROLSQ, to restore geometry that was distorted by XPLOR and to place solvent molecules. After 38 cycles of PROLSQ, the refinement converged to yield a model having an R value of 0.174 for the 12 397 reflections between 6 and 1.74 Å for which $F_o/\sigma > 1.5$.

RESULTS

Crystallography. The geometry of the refined model is reasonable (see Table I). The final ΔF map has a standard deviation of 0.047 electron/Å^3; it contains no peaks greater than 0.24 electron/Å^3 and only one peak lower than −0.24 electron/Å^3. This negative peak falls on the side chain of Lys-64, which is partially disordered. Inspection of $2F_o - F_c$ maps shows excellent electron density for all parts of the model, except residues 45–50. In this region, density is poor (from Lys-45 to Pro-47) or nonexistent (Lys-48 to Gly-50). Rough estimates of the coordinate errors in the model were obtained by the methods of Cruickshank (1949, 1954) and Luzatti (1952); these methods yield values for the overall rms coordinate error of 0.25 and 0.20 Å, respectively (data not shown). Since the density for residues 45–50 is poor, the refinement procedure results in high B values being assigned to these residues; these high B values cause large error estimates to be calculated for these residues in the Cruickshank coordinate error calculation. Omitting these residues from the calculation yields a revised estimate of 0.18 Å for the rms coordinate error, in good agreement with the results of the Luzatti method.

Comparison of Mutant and Wild-Type Backbones. The refined E43D/Ca^{2+}/pdTp ternary complex structure was compared to the refined wild-type ternary complex structure (Loll & Lattman, 1989) by several methods. Inspection of the models' gross features reveals obvious differences in the backbone conformation between residues 42 and 53; elsewhere, the models appear similar. Least-squares superposition (Kabsch, 1978) was used to place residues 7–41 and 54–141 of the mutant upon the corresponding residues in the wild type.[3] The rms Cα–Cα distance after superposition for these

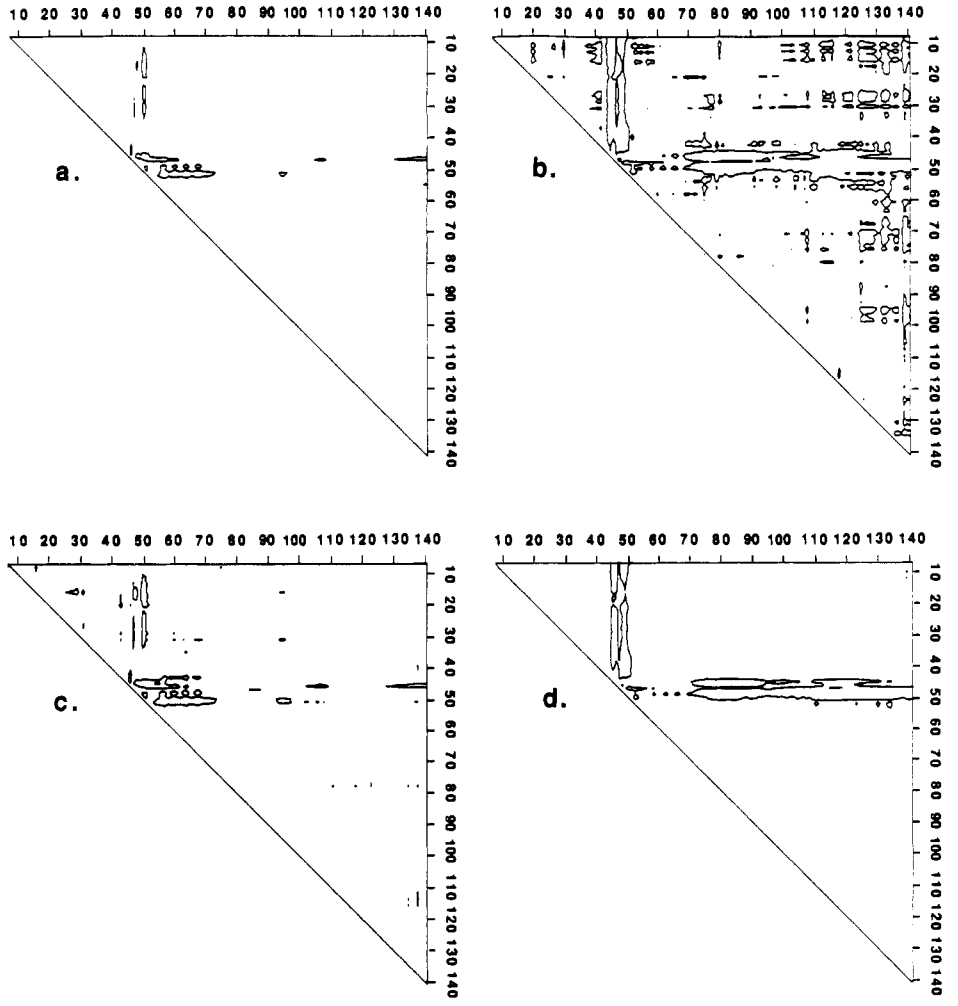

FIGURE 2: Difference distance matrix constructed by subtracting the distance matrix for the refined E43D/Ca^{2+}/pdTp structure from that of the refined wild-type/Ca^{2+}/pdTp structure. Contour levels used are as follows: (a) −0.50 Å, (b) −0.25 Å, (c) +0.25 Å, and (d) +0.50 Å. The matrix was calculated from α-carbon positions only. The scales at the top and side of each panel represent residue numbers.

two groups of residues was 0.16 Å; given the level of error expected in the coordinates, this might suggest that in these regions the backbones are essentially identical. However, inspection of a plot of Cα–Cα distance versus residue number (see Figure 1) reveals, in addition to the huge peak between residues 41 and 54, several small peaks that appear to rise above the noise of the plot, indicating conformational differences that may be significant and are not merely due to errors in the refined coordinates. Also, from Figure 1 it can be seen that the distance between corresponding α-carbons tends to increase in the last 30 residues of the molecules.

To further compare the mutant and wild-type protein backbones, we calculated a difference distance matrix in which the distance matrix for the mutant structure was subtracted from that of the wild type (Kundrot & Richards, 1987). This difference distance matrix is displayed in Figure 2 as a series of contour plots. In addition to the large differences already noted in the 41–54 loop, many small differences are noted, particularly in the C-terminal region.

Comparison of Active Site Structures. Residue 43 resides in the active site, and significant changes are found in the active site of the E43D mutant protein (see Figure 3). The overall arrangement of the mutant active site is similar to that of the wild-type ternary complex, but the two structures differ in several important details. The side chain of Asp-43 points out of the active site, toward the solution; in the wild type, Glu-43 reaches back into the active site. A water molecule is observed in the wild type bridging Glu-43 and the 5′-phosphate of the pdTp molecule. This molecule, which is thought to be an excellent candidate for the attacking nucleophile in the productive complex of enzyme, metal, and substrate, is completely absent from the E43D structure. In addition to the putative nucleophile, four other water molecules, out of the eight that are evident in the wild-type active site, are missing from the mutant active site.[4] In the wild-type

[3] The transformation matrix used to place the E43D structure upon the wild-type structure is as follows:

$$x_t = 0.999987(x - x_{cen}) + 0.001967(y - y_{cen}) - 0.004640(z - z_{cen}) + 4.94$$

$$y_t = -0.001948(x - x_{cen}) + 0.999984(y - y_{cen}) + 0.004196(z - z_{cen}) + 23.59$$

$$z_t = 0.004648(x - x_{cen}) - 0.004187(y - y_{cen}) + 0.999980(z - z_{cen}) + 14.14$$

where x, y, and z are the coordinates of the refined E43D structure, x_t, y_t, and z_t are the coordinates of the E43D structure superimposed upon the wild type, and the center of mass of the refined E43D structure is given by

$$x_{cen} = 5.01,\ y_{cen} = 23.88,\ z_{cen} = 14.51$$

All coordinates are expressed in angstrom units.

[4] More water molecules were located in the wild-type ternary complex structure than in the E43D ternary complex (82 vs 60), perhaps because the wild type has been refined to a lower R value. However, four of the five water molecules missing from the E43D active site have low B values in the wild type, and their absence from the mutant is therefore probably not due simply to a higher noise level in the mutant structure.

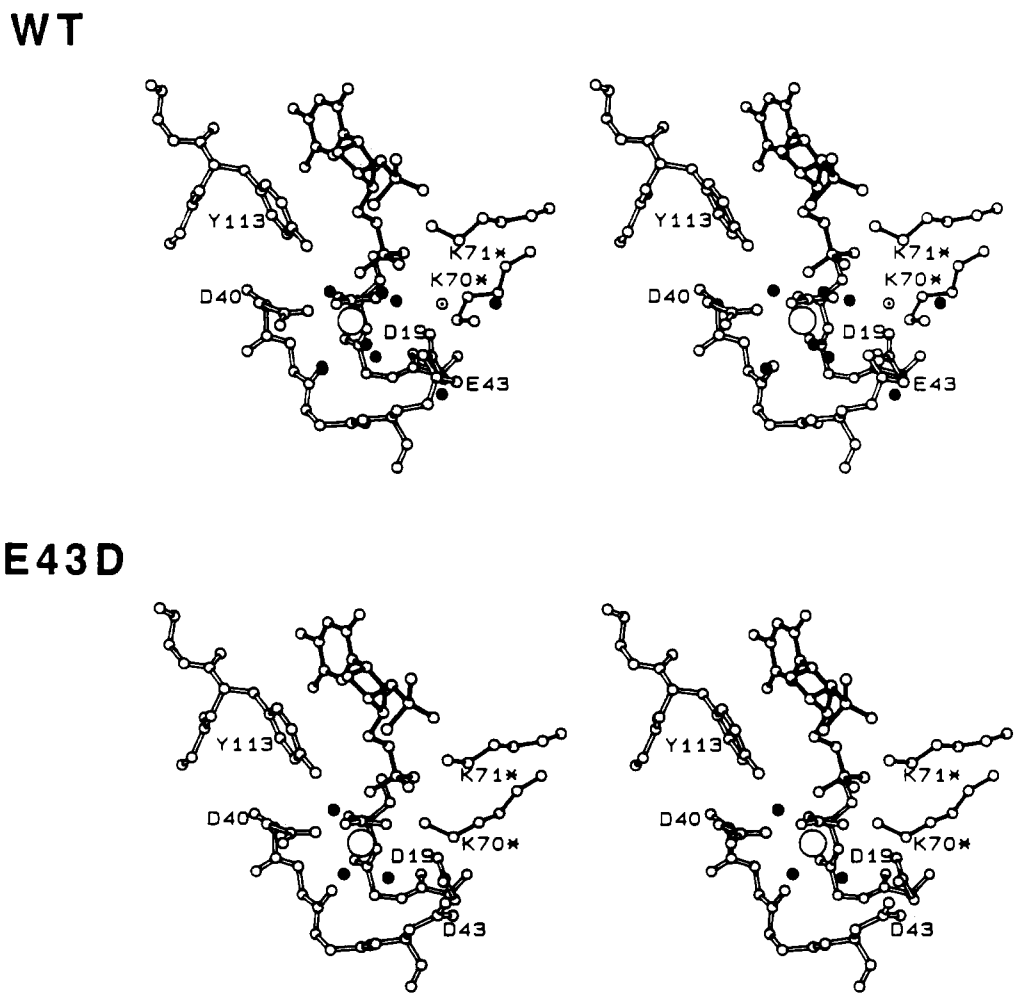

FIGURE 3: Active sites of the wild-type and E43D ternary complex structures. The pdTp molecule is seen at the top center of each figure (dark bonds); the calcium ion is represented by the large ball below the pdTp. Water molecules are shown as dark circles, except for the putative nucleophile in the wild-type structure, which is shown as a light circle with a dot in the center. Lysines 70 and 71, each marked with an asterisk to indicate it is derived from a symmetry-related molecule, can be seen at the right side of the figure. Nine water molecules can be seen in the wild-type figure; eight are in the active site, and the ninth bridges the first part of the mobile loop to the main body of the protein (this ninth water is visible below and to the right of E43 in the figure). The bridging water and five of the active site water molecules are not seen in the mutant active site.

structure, the missing water molecules are all seen to be part of one hydrogen-bonded network that is stabilized by hydrogen bonds with the γ-carboxylate of Glu-43 and with the 5′-phosphate of the inhibitor. One weakly occupied water site not found in the wild-type active site has been found in the mutant near the side chain of Asp-43.

One of the water molecules missing from the E43D active site is a ligand of the calcium ion in the wild-type structure; in the mutant, it has been displaced by the side chain of Lys-70 from an adjacent molecule in the crystal lattice. Side chains of symmetry-related lysines 70 and 71 have also been shown to protrude into the active site of the wild-type structure. The symmetry-related Lys-71 occupies the same position in the mutant and wild-type structures, situated between the 3′- and 5′-phosphates of the inhibitor. The position of the symmetry-related Lys-70 is quite different between the two structures, however. In the wild type, this lysine is involved in a salt bridge with Glu-43; in the E43D mutant, the side chain of residue 43 has been moved too far away to interact with this lysine, so the lysine has moved into a salt bridge with Asp-21, displacing a water ligand of the metal in the process. It is unclear whether this lysine's amino group has actually replaced the water as a ligand. The metal–nitrogen distance in the mutant is 3.5 Å, however, so it seems likely that, even if the lysine cannot be considered a ligand of the calcium, it has undergone a shift in pK so that in the crystal it is present as the uncharged form.

In the wild type, the ligands of the calcium ion are arranged in a distorted octahedral geometry with four equatorial ligands, one polar ligand "above" the metal, and two polar ligands sharing the position "below" the metal. This geometry is essentially preserved in the mutant, even though one of the equatorial ligands has been displaced by the symmetry-related Lys-70. The metal ion to ligand distances are slightly larger in the mutant than in the wild type (mean increase in metal–ligand distance = 0.13 Å), and the temperature factor of the calcium ion is higher in the mutant structure (in the wild type, the B factor of the Ca^{2+} is 6 Å^2 below the mean B factor of the structure; in the E43D mutant, the Ca^{2+} B factor is 7 Å^2 above the mean). Taken together, these facts indicate that the metal ion is less tightly localized in the mutant structure and occupies a slightly larger "cage". This is consistent with the changes that are seen to follow from the alteration of the side chain of residue 43, namely, the displacement of one the metal's ligands by a symmetry-related Lys-70 and the destabilization of other ligands by the removal of part of the hydrogen-bond network formed with water molecules and Glu-43.

Changes in the Loop between Residues 41 and 54. The loop comprising residues 41–54 (the "mobile loop") occupies very different conformations in the E43D and wild-type ternary

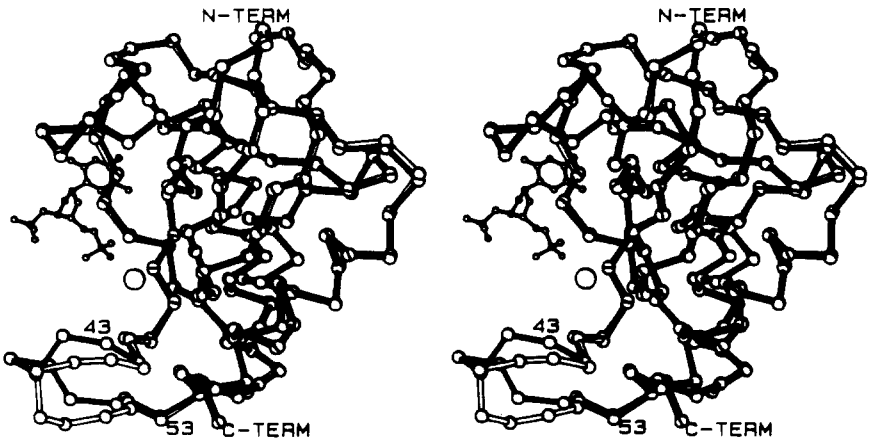

FIGURE 4: α-Carbon backbones of the wild-type and E43D mutant proteins, superimposed (wild type, dark bonds; E43D, light bonds). The amino and carboxyl termini of the protein are marked for reference, as are residues 43 and 53. The pdTp molecule and calcium ion are also included in this figure. The mobile loop, which differs significantly between the two structures, is seen at the lower left.

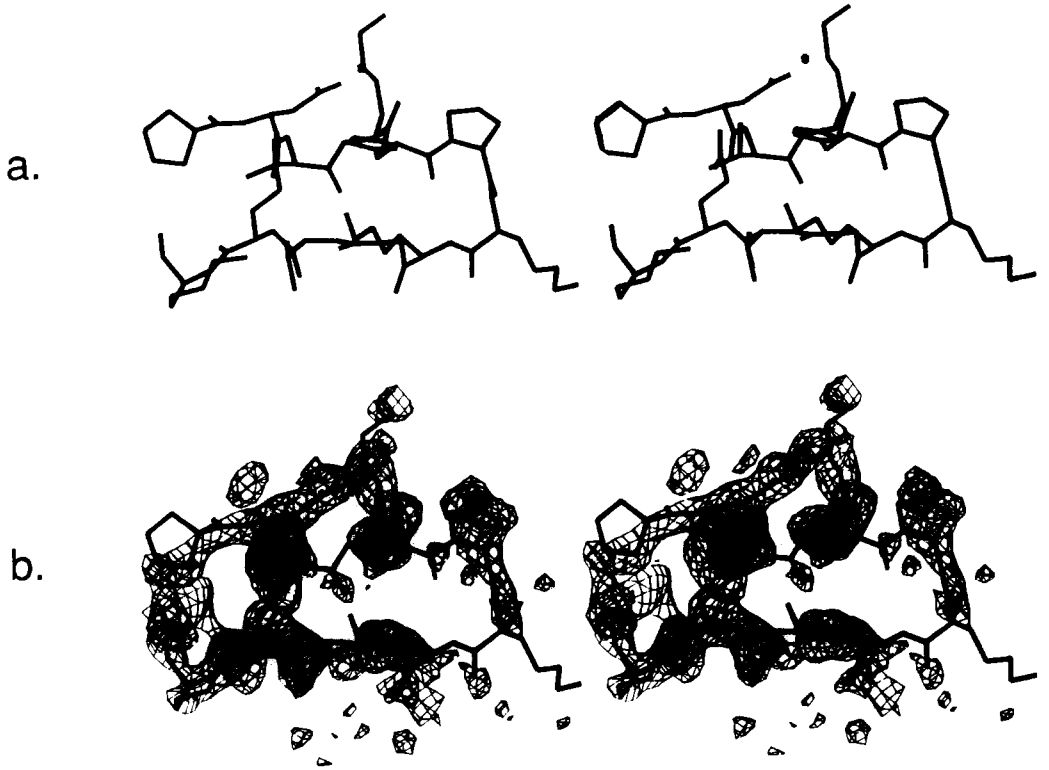

FIGURE 5: Stereo view of the electron density in the mobile loop region of the E43D mutant structure. (a) Refined model only. The chain begins at Pro-42 at the upper left, runs horizontally across the page, and then doubles back to Lys-53 at the lower left. Sequence of the section shown is as follows: PDTKHPKKGEK. (b) Refined model superimposed on electron density map. Map shown is a $2F_o - F_c$ map, with phases calculated from the final refined model, contoured at 0.7 standard deviation.

complex structures (see Figure 4). The backbone conformations are roughly similar through residue 43. The differences become more pronounced in residues 44 and 45, and at His-46 the two structures diverge completely and do not begin to converge again until Val-51. Through residues 52 and 53 the two chains become more similar, until, at Tyr-54, they become essentially superimposable.

As was noted earlier, the electron density is poor or nonexistent throughout parts of the mobile loop of the E43D structure (see Figure 5). It is important to explain, then, how we can be confident that the loop occupies different conformations in the mutant and wild-type structures.

The $2F_o - F_c$ maps show fair to good electron density for the wild-type backbone throughout the mobile loop (Figure 6). This electron density is not of the same high quality as that of the rest of the wild-type structure, and the mobile loop residues exhibit large temperature factors, indicating that static and/or temporal disorder is present throughout this loop, but we are confident that we can trace the path of the polypeptide chain of the wild-type mobile loop. For the E43D structure, we observe good electron density up to and including Thr-44; good density resumes at Val-51. Poor density is seen for residues 45–47; residues 48–50 are essentially out of density altogether. At residue 44, where the mutant polypeptide exits good density, it is heading in a different direction than the wild-type chain; at residue 51, where the mutant reenters good density, it is seen to have come from a different direction than the wild type. While the density for residues 45–47 of the mutant is not of high quality, the conformation we have built is at least consistent with the density; the wild-type conformation is not consistent with the density, nor can it be made consistent by small adjustments to backbone dihedral angles.

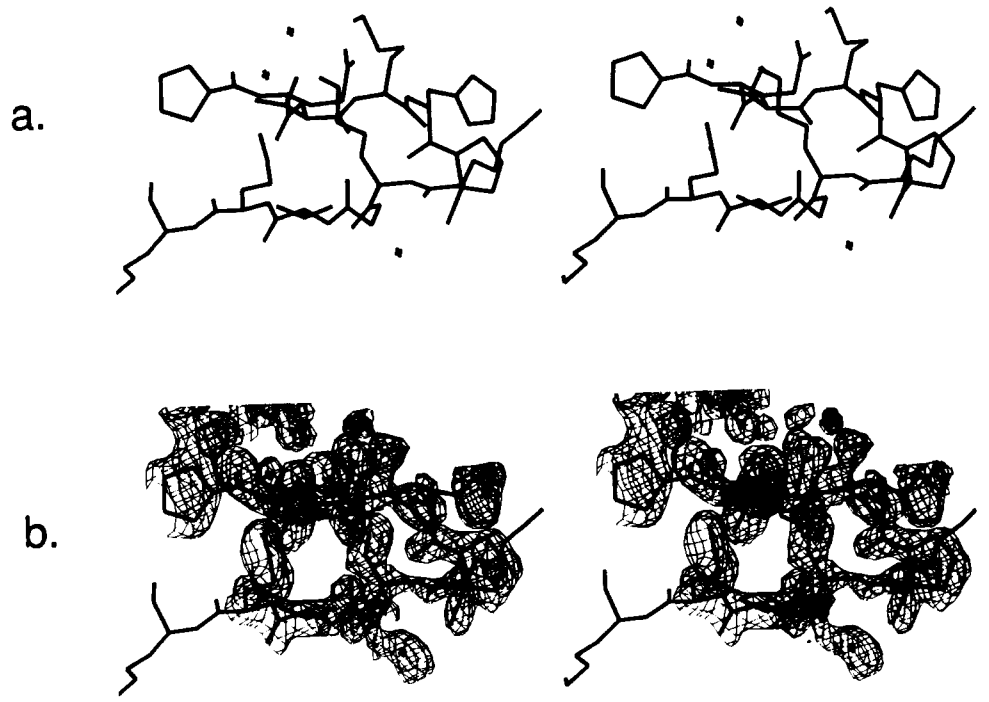

FIGURE 6: Stereo view of the electron density in the mobile loop region of the wild-type structure. (a) Refined model only. Orientation of the model is similar to that shown in Figure 5. (b) Refined model superimposed on the final $2F_o - F_c$ map, contoured at 1.0 standard deviation.

Examination of the refined structures reveals how the Glu-43 → Asp substitution can give rise to the large changes found in this mobile loop. In the ternary complex of wild-type enzyme, Ca^{2+}, and pdTp, Glu-43 interacts with the backbone amide protons of Lys-45 and His-46, stabilizing the conformation of the first part of the mobile loop. A water molecule inserted between the mobile loop and the body of the protein bridges the side chains of Thr-44 and Asp-19, also stabilizing this part of the loop. The Asp-43 side chain in the mutant cannot reach the position occupied by Glu-43 in the wild-type; thus, there is no reason for the polypeptide chain in the loop to pull away from the body of the protein, since Asp-43 cannot make the contacts with the amide protons of residues 45 and 46. The beginning part of the mutant loop is therefore closer to the body of the protein. Because of this motion of the mobile loop toward the protein and because of the position occupied by the side chain of Asp-43, the cavity that in the wild type is occupied by the water molecule bridging residues 44 and 19 shrinks in the mutant and becomes too small to admit this bridging water. Thus, the first half of the mobile loop has lost several stabilizing interactions and has gained no new interactions to offset this loss. This may well explain why the loop is less ordered in the E43D structure than in the wild-type structure.

Discussion

Differences in Backbone Conformation. It is clear that the polypeptide conformation between residues 41–54 differs drastically between the wild-type and E43D mutant structures. Less clear, however, is whether the small conformational differences seen at other points remote from the active site are significant or whether they are artifactual, due to coordinate error, slight differences in crystal packing or mother liquor composition, etc. As seen in Figure 2, widespread differences of the order of 0.25 Å exist between the mutant and E43D α-carbon positions. This is close to the estimated rms coordinate error of 0.18–0.20 Å; however, these error estimates are for all atoms, including flexible side chains, whereas the differences illustrated in Figure 2 are for α-carbon atoms only, whose positions should be relatively well determined. It is noteworthy that the backbone conformation of the E43D model refined from the first data set is quite similar to that of the final model refined against the second data set; small differences are seen distributed randomly throughout the polypeptide chain, but the two mutant structures resemble each other much more closely than either resembles wild type (data not shown). The second mutant is, of course, not completely independent of the first; however, we believe that the simulated annealing step separating them should remove most model bias.

If the small changes in the backbone throughout the structure indeed reflect global rearrangements due to the mutation, it is not clear how they are effected. It seems prudent to reserve judgement on these questions until a larger number of refined mutant nuclease structures is in hand.

Active Site Changes. The ratio of V_{max}/K_m for the E43D mutant is 1400-fold lower than that of the wild-type enzyme (Hibler et al., 1987). The mechanism that has been proposed for the wild-type enzyme (Cotton et al., 1979) requires that the γ-carboxylate group of Glu-43 acts as a general base, facilitating the attack of water on the scissile phosphodiester bond. This mechanism is fully consistent with work from the laboratory of Gerlt, showing that the reaction proceeds with inversion of configuration at the chiral phosphorus atom (Mehdi & Gerlt, 1982). In the wild type, the putative nucleophilic water is part of a network of water molecules hydrogen bonded both to the γ-carboxylate of Glu-43 and to the 5′-phosphate of the inhibitor. This water molecule is missing from the active site of the E43D/Ca^{2+}/pdTp complex. The side chain of Asp-43 in the mutant enzyme is not long enough to reach into the active site to help anchor the network of hydrogen-bonded water molecules; as a result, the water network is destabilized, and five of the eight water molecules found in the wild-type active site are missing from the E43D active site. A simple-minded mechanistic interpretation of the structural data, then, is that the reduction of activity in the E43D mutant is due to two related factors: (1) the loss of general-base catalysis, because the shortened side chain of Asp-43 cannot reach into the active site and act as a general

base, and (2) the absence of a securely positioned water network, including a water molecule that can act as a nucleophile.

This interpretation is consistent with the refined structures of the wild-type and E43D ternary complexes. However, we must note several points that emerge from the structure analysis which may bear on any mechanistic interpretation. For example, it appears that the calcium ion in the mutant structure is held less tightly in position than that in the wild type. However, the K_a for calcium for the mutant is actually slightly lower than that for the wild-type enzyme. Taken together, these facts could mean several things: Rigid positioning of the calcium may interfere with efficient catalysis, and the looser calcium positioning of the mutant partially makes up for its catalytic shortcomings. Another explanation is that the K_a determined in the presence of an actual substrate (DNA) has little bearing on the structure presented here, which is that of a nonproductive complex of enzyme, metal, and inhibitor. A third possibility is that the detailed nature of the metal binding is not crucial to catalysis, and the differences in metal binding observed in the two structures are not germane to discussions of mechanism.

Another fact to bear in mind when drawing mechanistic conclusions from the active site structure is the observation of two radically different conformations of the mobile loop adjoining the active site in the wild-type and E43D structures. This loop is not seen to interact with the mononucleotide inhibitor bound in the active site, but it is possible that the loop does interact with the large nucleic acid polymers that are substrates for the enzyme. Thus, the reduced catalytic activity of the E43D mutant may be in part due to this altered loop conformation.

A third reason to be cautious about the mechanistic implications of this structure is the strong crystal contact that brings two lysine side chains from a molecule in an adjacent unit cell into the enzyme's active site. Any mechanistic conclusions are based on the assumption that the conformation of the mononucleotide pdTp in the enzyme active site is similar to that of an actual substrate undergoing hydrolysis. However, one of the two symmetry-related lysines makes strong hydrogen bonds with both of the phosphate groups of the inhibitor; the other lysine has changed positions in going from the wild-type structure to the mutant, in response to the altered active site environment. In the E43D structure, this lysine has displaced a water ligand of the metal ion in order to hydrogen bond with Asp-21 and the 5′-phosphate of the inhibitor.

The ambiguities posed by the intermolecular contacts, the variable loop conformation, and other points are now being attacked experimentally from a number of directions. More precise answers should become available in due course.

Comparison with NMR Results. NMR experiments performed in solution have led investigators to conclude that nuclease E43D undergoes conformational rearrangements at sites remote from the site of the mutation (Wilde et al., 1988). Side chains suggested to undergo rearrangements in the mutant include Leu-25, Phe-34, Val-74, and Phe-76. In our E43D and wild-type crystal structures, the conformations of these side chains are identical. The changes seen in NMR spectra imply shifts of less than 0.5 Å in the side-chain atoms, close to the uncertainty in the X-ray coordinates. It may be, however, that the molecule adopts different conformations in solution and in the crystal. The reasons for these differences, as well as their exact nature, are unknown. Possible contributing factors include the constraints imposed by the crystal lattice, which may select for wild-type-like conformers during crystallization, and differences in solution conditions such as pH, temperature, and the presence or absence of various solutes between the NMR experiments and the crystallization experiments. Solid-state NMR experiments may offer a means of checking the disparity observed between the solution NMR and single-crystal diffraction experiments.

Summary. The refined high-resolution structure of the ternary complex of nuclease E43D, Ca^{2+}, and pdTp reveals that the structure of the mutant enzyme differs from that of the wild type in several important ways. The Asp-43 side chain fails to fulfill several of the functions of Glu-43 in the wild-type protein, including (1) acting as a general base during catalysis, (2) stabilizing an active site network of eight hydrogen-bonded water molecules seen in the wild type, which is shown to be reduced to merely three water molecules in the mutant active site (one of the missing water molecules may represent the nucleophile active in nucleic acid hydrolysis), and (3) stabilizing the mobile loop comprising residues 42–53 by interacting with the protein backbone at positions 45 and 46. In addition, a water molecule bridging the mobile loop to the main body of the wild-type protein is excluded from the mutant structure, further destabilizing the conformation of this loop.

The essential calcium ion appears to be less tightly constrained within its binding site in the mutant enzyme than in the wild type. The coordination sphere of this metal ion has been perturbed in the mutant by an alteration in a crystal contact caused by the mutation.

While the crystal structure of the mutant enzyme differs significantly from that of the wild type, small differences inferred from solution NMR experiments are not seen in the crystal structures.

The magnitude and number of changes caused by the apparently small change of a glutamic acid to an aspartic acid suggest that mechanistic interpretation of the altered hydrolytic activities of nuclease mutants will not be simple; naive model-building experiments conducted without structural data are unlikely to yield correct results.

Acknowledgments

Part of the diffraction data used in this study were collected at Brookhaven National Laboratory in the Biology Department's single-crystal diffraction facility at the National Synchrotron Light Source. This facility is supported by the U.S. Department of Energy. Film data were processed at the National Science Foundation Macromolecular Computing Facility at Purdue University. We thank Tim Schmidt for generous assistance during data processing, John Gerlt for supplying the plasmid pONF1 and for helpful discussions, and Phil Bolton and Dennis Torchia for sharing results and supplying useful insights into NMR methodology.

References

Brunger, A. T. (1988) *J. Mol. Biol. 203*, 803.
Brunger, A. T. (1989) *Acta. Crystallogr. A45*, 50.
Cotton, F. A., Hazen, E. E., Jr., & Legg, M. J. (1979) *Proc. Natl. Acad. Sci. U.S.A. 76*, 2551.
Cruickshank, D. W. J. (1949) *Acta Crystallogr. 2*, 65.
Cruickshank, D. W. J. (1954) *Acta Crystallogr. 7*, 519.
Hendrickson, W. A. (1985) *Methods Enzymol. 115*, 252.
Hibler, D. W., Stolowich, N. J., Reynolds, M. A., Gerlt, J. A., Wilde, J. A., & Bolton, P. H. (1987) *Biochemistry 26*, 6278.
Howard, A. J., Gilliland, G. L., Finzel, B. C., Poulos, T. L., Ohlendorf, D. H., & Salemme, F. R. (1987) *J. Appl. Crystallogr. 20*, 383.
Kabsch, W. (1978) *Acta Crystallogr. A34*, 827.

Kundrot, C. E., & Richards, F. M. (1987) *J. Mol. Biol. 193*, 157.
Loll, P. J., & Lattman, E. E. (1989) *Proteins: Struct., Funct., Genet. 5*, 183.
Luzatti, P. V. (1952) *Acta Crystallogr. 5*, 802.
Mehdi, S., & Gerlt, J. A. (1982) *J. Am. Chem. Soc. 104*, 3223.
Sheriff, S., & Hendrickson, W. A. (1987) *Acta Crystallogr. A43*, 118.
Steigemann, W. (1974) Die Entwicklung und Anwendung von Rechenverfahren und Rechenprogrammen zur Stukturanalyse von Proteinen am Beispiel des Trypsin-Trypsinhibitor Komplexes, des freien Inhibitors und der L-Asparaginase, Ph.D. Thesis, Technical University of Munich.
Takahara, M., Hibler, D. W., Barr, P. J., Gerlt, J. A., & Inouye, M. (1985) *J. Biol. Chem. 260*, 2670.
Wilde, J. A., Bolton, P. H., Dell'Acqua, M., Hibler, D. W., Pourmotabbed, T., & Gerlt, J. A. (1988) *Biochemistry 27*, 4127.

Solid-State ^{13}C and ^{15}N NMR Study of the Low pH Forms of Bacteriorhodopsin†

Huub J. M. de Groot,‡,§,‖ Steven O. Smith,‡,⊥ Jacques Courtin,§ Ellen van den Berg,§ Chris Winkel,§ Johan Lugtenburg,§ Robert G. Griffin,‡ and Judith Herzfeld*,‖

Francis Bitter National Magnet Laboratory, Massachusetts Institute of Technology, Cambridge, Massachusetts 02139, Gorlaeus Laboratoria der Rijksuniversiteit te Leiden, 2300 RA Leiden, The Netherlands, and Department of Chemistry, Brandeis University, Waltham, Massachusetts 02254

Received September 11, 1989; Revised Manuscript Received February 13, 1990

ABSTRACT: The visible absorption of bacteriorhodopsin (bR) is highly sensitive to pH, the maximum shifting from 568 nm (pH 7) to ~600 nm (pH 2) and back to 565 nm (pH 0) as the pH is decreased further with HCl. Blue membrane (λ_{max} >600 nm) is also formed by deionization of neutral purple membrane suspensions. Low-temperature, magic angle spinning ^{13}C and ^{15}N NMR was used to investigate the transitions to the blue and acid purple states. The ^{15}N NMR studies involved [ϵ-^{15}N]lysine bR, allowing a detailed investigation of effects at the Schiff base nitrogen. The ^{15}N resonance shifts ~16 ppm upfield in the neutral purple to blue transition and returns to its original value in the blue to acid purple transition. Thus, the ^{15}N shift correlates directly with the color changes, suggesting an important contribution of the Schiff base counterion to the "opsin shift". The results indicate weaker hydrogen bonding in the blue form than in the two purple forms and permit a determination of the contribution of the weak hydrogen bonding to the opsin shift at a neutral pH of ~2000 cm^{-1}. An explanation of the mechanism of the purple to blue to purple transition is given in terms of the complex counterion model. The ^{13}C NMR experiments were performed on samples specifically ^{13}C labeled at the C-5, C-12, C-13, C-14, or C-15 positions in the retinylidene chromophore. The effects of the purple to blue to purple transitions on the isotropic chemical shifts for the various ^{13}C resonances are relatively small. It appears that bR_{600} consists of at least four different species. The data confirm the presence of 13-*cis*- and *all-trans*-retinal in the blue form, as in neutral purple dark-adapted bR. All spectra of the blue and acid purple bR show substantial inhomogeneous broadening which indicates additional irregular distortions of the protein lattice. The amount of distortion correlates with the variation of the pH, and not with the color change.

Bacteriorhodopsin (bR),[1] the purple membrane protein of the halophilic bacterium *Halobacterium halobium* (Oesterhelt & Stoeckenius, 1971, 1973a; Lozier et al., 1975), works as a light-driven proton pump, establishing a proton gradient across the cell membrane [for a review, see, e.g., Stoeckenius and Bogomolni (1982)]. While the detailed 3D structure of bR is unknown, it has been established that the protein consists of a single polypeptide chain (Khorana et al., 1979; Ovchinikov et al., 1977, 1979) that is believed to be folded into seven transmembrane segments (Henderson & Unwin, 1975) surrounding the retinylidene chromophore.

One of the remarkable features of bR is the relatively large (5100 cm^{-1} at neutral pH) protein-induced shift of the absorption maximum (λ_{max}) of the chromophore, which is responsible for its characteristic purple color. This spectral shift, commonly referred to as the opsin shift, is defined as the

† This research was supported by the National Institutes of Health (GM-23289, GM-36810, and RR-00995), the "stichting Scheikundig Onderzoek Nederland" (SON, Netherlands Foundation for Chemical Research), and the "Nederlandse Organisatie voor Wetenschappelijk Onderzoek" (NWO, Netherlands Organization for the Advancement of Scientific Research). H.J.M.d.G. is a recipient of an NWO fellowship (S81-346) and a research career development fellowship (Akademie-Onderzoeker) from the "Koninklijke Nederlandse Akademie van Wetenschappen (Royal Dutch Academy of Sciences). S.O.S. was supported by an NIH postdoctoral fellowship (GM-10502).

‡ Massachusetts Institute of Technology.
§ Gorlaeus Laboratoria der Rijksuniversiteit te Leiden.
‖ Brandeis University.
⊥ Present address: Department of Molecular Biophysics and Biochemistry, Yale University, New Haven, CT 06511.

[1] Abbreviations: bR, bacteriorhodopsin; bR_{560}, dark-adapted bR comprising a mixture of bR_{555} and bR_{568} (Scherrer et al., 1989); bR_{555}, 13-cis component of dark-adapted bR; bR_{568}, light-adapted bR; bR_{600}, blue membrane obtained by acidification or deionization of bR_{560}; bR_{565}, acid purple membrane obtained by acidification of blue membrane with HCl; CP, cross-polarization; *f*, fraction of total intensity in the difference spectrum; FWHM, full width at half-maximum; MAS, magic angle spinning; PSB, protonated Schiff base; PM, purple membrane; ppm, parts per million; TMS, tetramethylsilane; λ_{max}, wavelength of maximum visible absorption; ω_r, magic angle spinning speed; σ, chemical shift.

0006-2960/90/0429-6873$02.50/0 © 1990 American Chemical Society